Meshing generation strategy for prediction of ship resistance using CFD approach

Serliana Yulianti[1], S Samuel[1], T S Nainggolan[1] and Muhammad Iqbal[2]

[1]Department of Naval Architecture, Faculty of Engineering, Diponegoro University, Semarang, 50275, Indonesia
[2]Department of Naval Architecture, Ocean, and Marine Engineering, University of Strathclyde, Glasgow, UK.

Coresponding author: samuel@ft.undip.ac.id

Abstract. CFD is a numerical approach used to solve fluid problems. In the CFD simulation process, the meshing stage is crucial to produce high accuracy. Meshing is a process where the geometric space of an object is broken down into many nodes to translate the physical components that occur while representing the object's physical shape. The research objective was to analyze the characteristics of the mesh technique in the *Finite Volume Method* (FVM) using the RANS (*Reynolds - Averaged Navier - Stokes*) equation. The numerical simulation approach used three mesh techniques, namely overset mesh, morphing mesh, and moving mesh. The k-ε turbulent model and VOF (*Volume of Fluid*) were used to model the water and air phases. The mesh technique approach in CFD simulation showed a pattern under experimental testing. This research showed the difference in value to the experimental results, namely by using the moving mesh method, the difference in resistance difference was 8% at high-speed conditions, the difference in trim value at overset mesh was 11%, and the difference in heave value with the moving mesh method was 14% at low speed. The conclusion reported that overset mesh had better than other mesh methods.

Keywords: CFD, Fridsma hull, morphing mesh, moving mesh, overset mesh

1. Introduction

An experiment conducted by G. Fridsma in 1969 has sparked many researchers to conduct similar research related to planing hulls. Fridsma conducted experimental analysis on ships with the planing type, hereinafter known as Fridsma ship, with several L/B configurations, displacement, deadrise angle, LCG (Longitudinal Center of Gravity), and so on [1]. Supported by the ship's simple geometry, until now, there has been much research discussing the Fridsma ship.

The rapid development of technology makes research more effective to do. One technology supporting the research of ships is a numerical simulation method based on Computational Fluid Dynamics (CFD). CFD is a system program that can plan and analyze an engineering product using mathematical solutions. In the analysis using CFD, especially ship type planing, the methods used to predict the resistance and movement of the planing hull included FVM (Finite Volume Method), FEM (Finite Element Method), FDM (Finite Difference Method), and analytical-experimental. According to Yousefi in 2013, the most appropriate method used to predict drag, trim, and heave on ships was FVM because

it produced better calculation accuracy than other methods [2]. In 2019, a numerical simulation using the FVM method was carried out on the Fridsma ship. The simulation explained that CFD could be used for ships with low speeds (Fr 0.59). However, at high speed (Fr 1.78), there was an inability to calculate numerically, requiring evaluation [3]. Research on the spray strips application has also been carried out on the Fridsma to reduce ship resistance. The innovation from this research has succeeded in increasing the performance of the Fridsma ship by reducing drag by up to 6% at high speed [4].
As for the meshing method, it is crucial to pay attention to the simulation process using CFD. The meshing techniques that researchers often use are the overset mesh[5], morphing mesh [6], and moving mesh[7]. In 2021, research was carried out on fridsma hull ships using an overset mesh system to reduce numerical ventilation problems [8]. Previously, research was conducted on the RBF (radial basis functions)-based grid morphing mesh system[9]. Furthermore, research was conducted on the characteristics of the moving mesh method [10]. In 2017, Agustino De Marco analyzed the hydrodynamics of the storied hull type using overset mesh and morphing mesh techniques to determine the two mesh techniques' characteristics[11]. Therefore, it is essential to study each mesh method on vessel as one of the parameters to improve calculation accuracy. In this research, the Fridsma hull ship was used to analyze each mesh technique characteristic.

2. Method

2.1 Research objects

Early research on the hydrodynamics of planing hulls has been started in the United States since 40 years ago [12]. Based on the Froude number value, ships can be classified based on the range, as shown in figure 1. In a planing type ship, the balance of the ship's weight was caused by the pressure acting on a wetted surface area. The pressure was composed of two components, namely hydrostatic, which related to buoyancy, and hydrodynamics relating to the ship's speed[13]. Therefore, a ship can be classified based on the pressure acting when moving as follows:

1. Displacement vessel, if the hydrostatic pressure was more significant than the hydrodynamic pressure.
2. Semi-displacement vessel, if the hydrostatic and hydrodynamic pressures were the same.
3. Planing vessel, if the hydrostatic pressure was less than the hydrodynamic pressure.

This research used experimental data Fridsma hull form as the research objects as described in Table 1 in calm water condition. The lines plan drawing of the Fridsma ship was described in Figure 2. In this research, the movement of the ship using DFBI used two degrees of freedom to simulate trim and heave.

Table 1. Experiment data by Gerard Fridsma [1]

Dimension	Unit	Value
L/B	-	5,00
L	m	1,143
B	m	0,229
TAP	m	0,081
LCG by AP	m	0,457
VCG by keel	m	0,067
τo	Degree	1,569
β	Degree	20,00
Δ	Kg	107,67
Iyy = Izz	Kg.m2	0,235

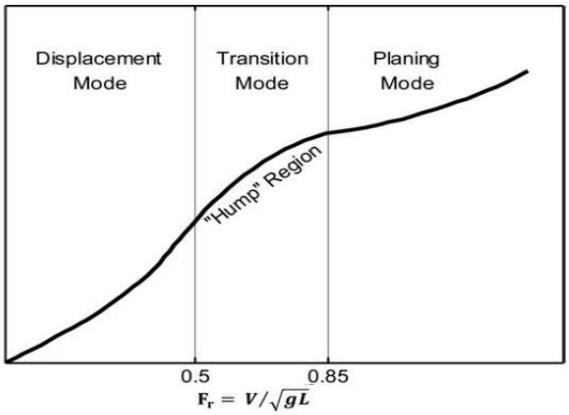

Figure 1. Ship classification based on froude number [14]

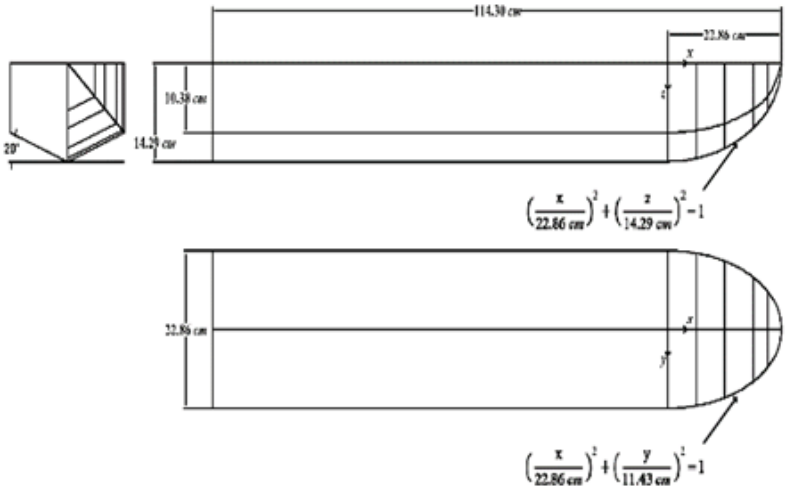

Figure 2. Lines plan of Fridsma hull form

2.2. Numerical method

CFD was developed to predict the shape of the flow without compromising the accuracy of the calculation. Every CFD program used mathematical equations to solve fluid flows. FVM is a CFD that represented and evaluated partial differential equations using RANS. The Reynolds averaged Navier-Stokes equation (RANS) defined the conservation laws of mass and momentum. The first discretization stage was to divide the computational domain into a finite number of volumes, forming a mesh. Next, the partial differential equations were integrated into each volume using the divergence theorem and producing an algebraic equation for each cell. In the cell center, the cell meant the variable flow value was stored at that node [15]. An essential goal of any CFD program was to solve equations using boundary and initial conditions. The RANS equation as in equation 1, was developed based on the concept that the speed and length of the ship described the turbulence effect around the hull. In the calculation, the k- ε turbulence model, which served as a wall, was used to describe the effect of turbulence on the flow[16].

$$\frac{\delta F}{\delta t}+\frac{\delta uF}{\delta x}+\frac{\delta vF}{\delta y}+\frac{\delta wF}{\delta z}=0 \quad (1)$$

Wall function (y+) divided the wall and the fluid flow. It served to capture the boundary layer, which played a vital role in calculating resistance. The value of y+ played a vital role in reducing calculation inaccuracies. Lotfi and Ahmed Gultekin researched to obtain accurate results. Lotfi used the value of y+

50 – 150 [17], and Ahmed Gultekin used a value of y+ 45-60 [18]. Meanwhile, in this research, the results obtained y+ 45-70. The calculation of y+ value was based on ITTC [19], which is as described in equation 2 as follow:

$$\frac{y}{L} = \frac{y^+}{Re\sqrt{Cf/_2}} \quad (2)$$

To determine the time-step in this research, the *Courant-Friedrichs-Lewy* (CFL) number was used. The CFL number indicated the number of points traveled by a fluid particle in a time interval. The faster the ship, the smaller the time-step that would be used. In this research, the time-step used was 0.009 s. The time-step referred to the ITTC calculation in equation 3, with *L* as the ship's length and *U* as the ship's speed.

$$\Delta t\ ITTC\ =\ 0{,}005 \backsim\ 0{,}01\ \frac{L}{U} \quad (3)$$

The dimensions of the towing tank in the CFD simulation followed the ITTC recommendations described in Figure 3, consisting of (a) overset mesh, (b) morphing mesh and moving mesh[19].

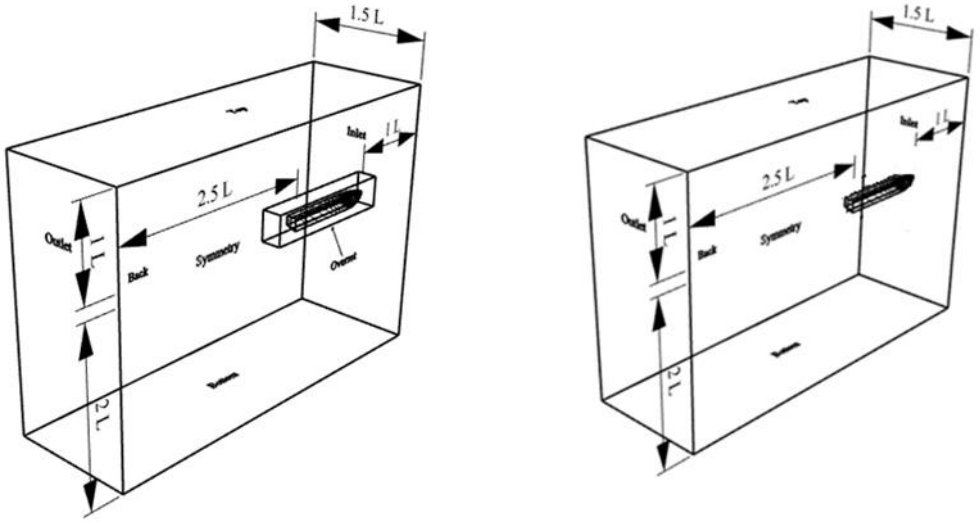

Figure 3. Fluid domain (a) overset mesh (b) morphing mesh and moving mesh.

The mesh density was centered on the hull and water surface so that the results remained accurate in a relatively faster computation time. In addition, refinement in the bottom area was needed for more accurate results. The local meshing was performed using the anisotropic mesh to focus on the x, y, or z ordinates. In this simulation, the mesh density was divided into several parts, as in Table 2 and Figure 4 visualize the surface mesh domain density.

Table 2. Mesh density

Parts	Type of Refinements	Size
Tank	Surface	0,7874 L
Water Surface Fine	Volume	0,0062 L
Water Surface Medium	Volume	0,0123 L
Water Surface Coarse	Volume	0,0246 L
Hull Box 1	Volume	0,0984 L
Hull Box 2	Volume	0,0492 L
Hull Box 3	Volume	0,0246 L
Hull Box 4	Volume	0,0123 L
Wake Fine	Volume	0,0492 L

Wake Medium	Volume	0,0984 L
Wake Coarse	Volume	0,1969 L
Hull	Surface	0,0030 L

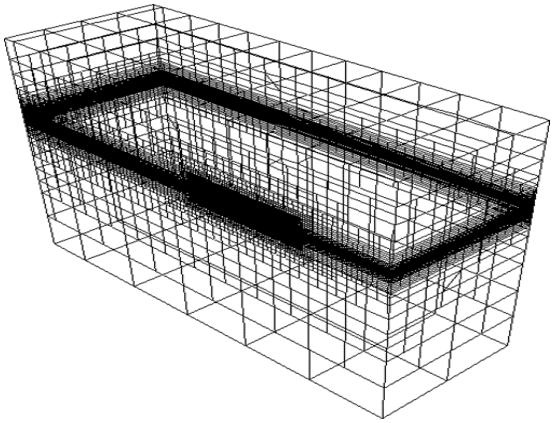

Figure 4. Mesh configuration

2.3 Overset mesh

Overset mesh was a mesh method using donor-acceptor cells, so there was an overset box and background, as shown in figure 5. This method required more than one geometry with a background as a donor and an overset as a donor-recipient. Active cells were found at each end of the geometry in the overset as an intermediary for donor-acceptor cells. There were passive cells in the background, replaced by overset cells. According to research conducted by Simon Manchini, the donor-cells variable can be calculated as in equation 4 [20]:

$$\varphi_{acceptor} = \sum \alpha_1 \varphi_1 \quad (4)$$

Where α_1 was the interpolation weighting factor, φ_1 was the dependent variable, and φ were acceptor donor cells. The overset mesh consisted of the background and the overset box, so the set-up for each geometry is shown in Table 3.

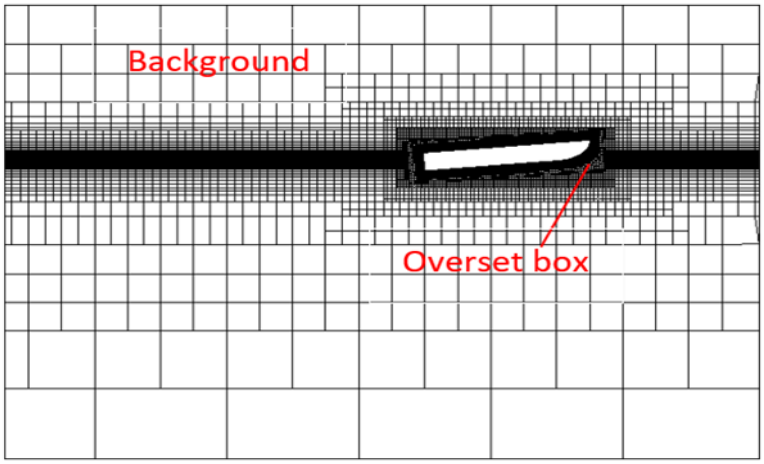

Figure 5. Background and overset box

Table 3. Setup on overset mesh

Part	Node	Properties	Set up
Background	Region, background, physic values	Motion specification	Stasioner
Overset box	Region, substract, physic values	Motion specification	DFBI rotation & translation

2.4 Morphing mesh

Morphing mesh was an interpolation technique that allowed a single object to change shape [21]. By creating an intermediate frame to the model, the intermediate form was produced indefinitely. In the ship cases, the entire hull could be transformed parametrically using the principal dimensions. Morphing mesh was suitable for complex relative motions, while more significant deformations might require new cells to maintain a high-quality mesh. Figure 6 is a visualization of the morphing mesh technique before deforming. The mesh morphing technique only used a towing tank geometry, different with overset mesh technique.

The morphing mesh technique required special treatment of moving nodes to control the accuracy of space derivatives and time-stepping schemes. It was done by interpolating the fluid flow variables precisely [22]. According to research conducted by Agustino De Marco, an interpolated field was used to replace mesh nodes based on the *Radial Basis Functions* (RBF) method. To generate the interpolated field, a system of equations was solved as in equation 5, using the control vertices and their defined displacements:

$$d'_i = \sum_{j=0}^{n} \lambda_j \sqrt{r_{ij}^2 + c_j^2} + \alpha \quad (5)$$

Where d'_i was the mesh displacement, i was every vertex of the mesh, λ_j was the coefficient of expansion, n was the number of cells, c_j was a fundamental constant, α was a constant value, and r_{ij} was the distance between two vertices. To get r_{ij} value, Agustino De Marco used the following equation 6:

$$r_{ij} = [\, x_i - x_j] \quad (6)$$

x_i was the difference in vertex distance x, and x_j was the vertex distance y. Table 4 was a set-up of the morphing mesh method using Star CCM software.

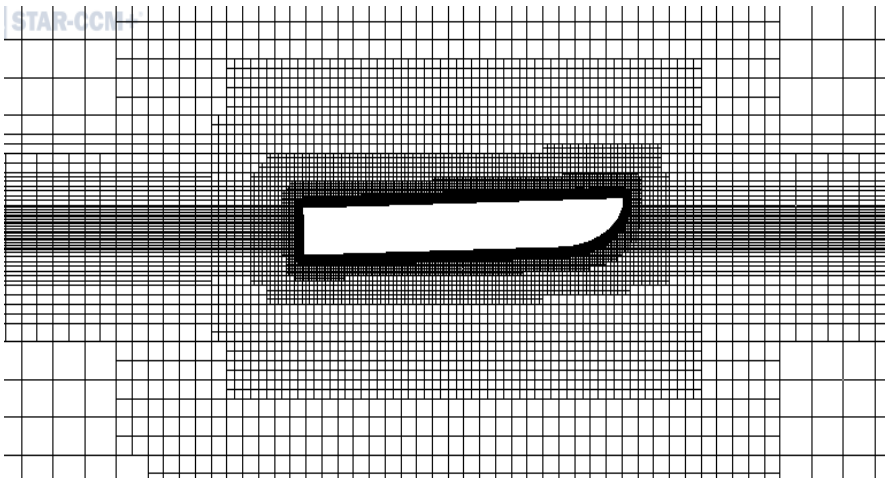

Figure 6. Morphing mesh before deformation

Table 4. Setup on morphing mesh.

Part	Node	Property	Set up
Background	Region, substract, physic values	Motion specification	DFBI morphing

2.5 Moving mesh

The moving mesh technique moved the entire grid according to the rigid motion of the ship. The grid itself was not altered but remained rigid. This approach had several advantages because only the flow variable must be corrected according to the ship motion, the method was excellent, and the computational error was small. This moving mesh technique differed from the morphing or overset mesh methods. The primary difference in this mesh technique was shown on the background movement and the ship as described in Table 5 and the visualization of Figure 7.

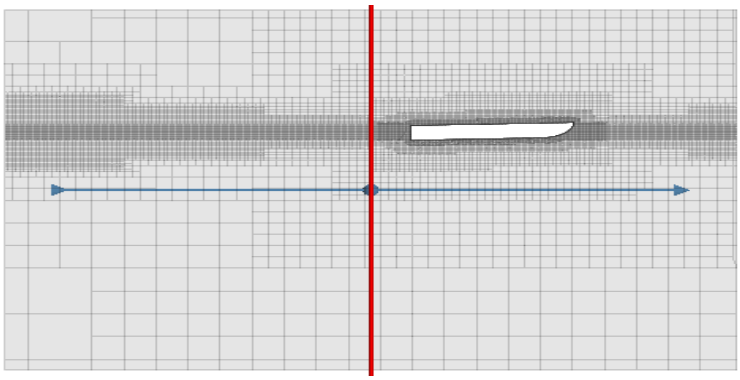

Figure 7. Moving mesh before analyzed

Table 5. Setup on moving mesh.

Bagian	Node	Properti	Set up
Background	Region, substract, physic values	Motion specification	DFBI rotation & translation

3. Result and Discussion

3.1 Overset mesh technique

Overset mesh was used to solve the equations of motion and rotation of objects, which occurred in solid objects interacting with fluids [21]. The overset mesh method was commonly used for numerical simulation of maneuver tests, roll decay tests, and estimating the ship's response to waves. In Figure 4, it can be seen how data transfer works from the overset mesh method. The meshing visualization can be seen in figure 8a, the overset mesh condition before running. Additionally, figure 8b shows the overset mesh condition after running. There were different positions in the overset section to translate the physical properties that worked, including the 2DOF motion of the ship. In figure 9, there were active cells at each end of the overset geometry as donor recipients and passive cells in the background, which were replaced by overset cells.

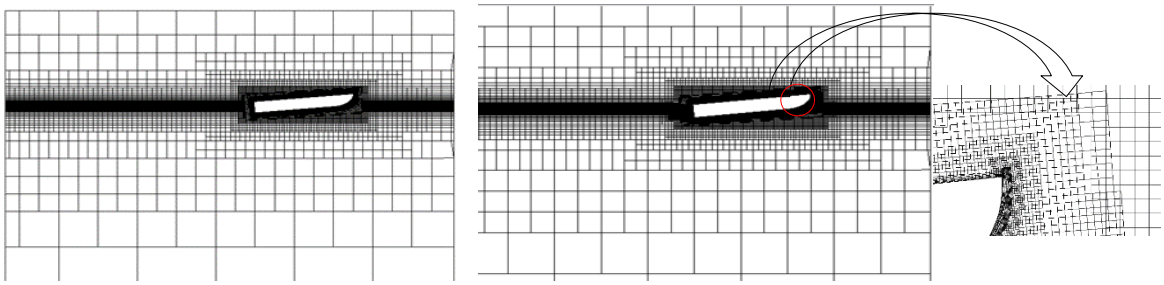

Figure 8. Overset mesh (a) before analyzed (b) after analyzed

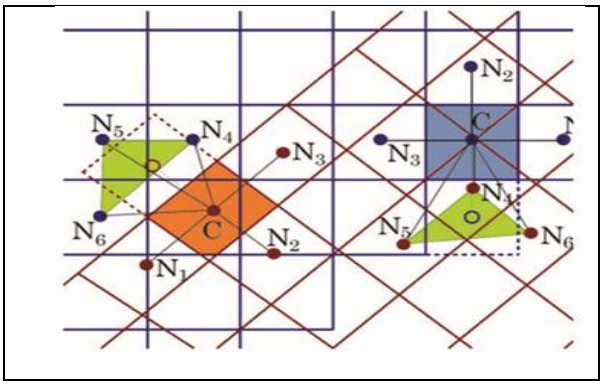

Figure 9. Data transfer visualization between overset mesh (red) and background mesh (blue), where acceptor cell (orange) received data from donor cell (green) [20].

3.2 Morphing mesh technique

Morphing mesh was a technique without movement of the ship's domain and background. Based on interpolation between two forms, morphing would require two model forms consisting of a source and a target so that the transformation could occur from the source to the target. No target model was available. Furthermore, one of the extreme models could be generated by applying Laplace coordinates. Morphing mesh was suitable for complex relative movements. The morphing mesh method was often used in the marine sector to analyze offshore or offshore buildings. Figure 10a is an image of the morphing mesh before deforming. Figure 10b shows that it has been deformed.

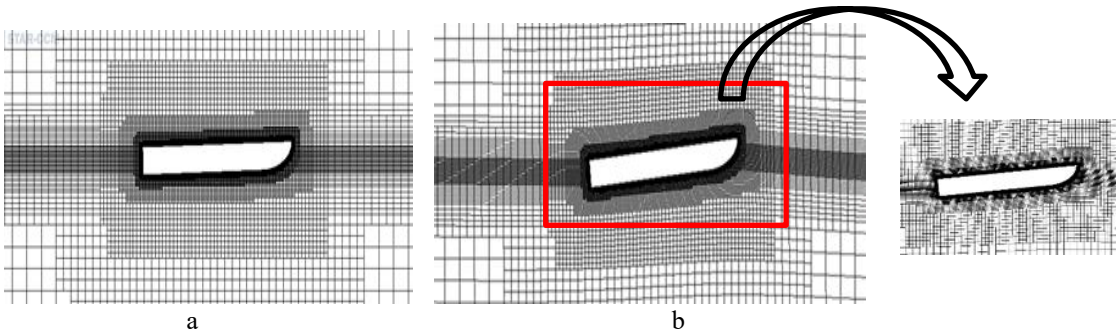

Figure 10. Morphing mesh (a) before deformation (b) after deformation

3.3 Moving mesh technique

In this method, the entire grid was moved according to the ship's motion. This approach had several advantages because only the flow variable had to be corrected according to the ship's motion. The method was excellent, and the computational error was small. On the other hand, this method only

applied to the motion of one rigid body. The moving mesh technique had two primary and significant weaknesses in testing the durability of the hull, namely the need to create a set-up-free surface where the background moves freely, and the object under investigation did not move. Other research on moving mesh has also been carried out for applications on CFD[22] . The second drawback was that it could cause additional oscillations or spurious waves that affected trim and sinkage, which could cause errors in the analysis. Figure 11 a is a visualization of the moving mesh before analysis. Figure 11b has a red box where the red box shows the occurrence of oscillations or false waves.

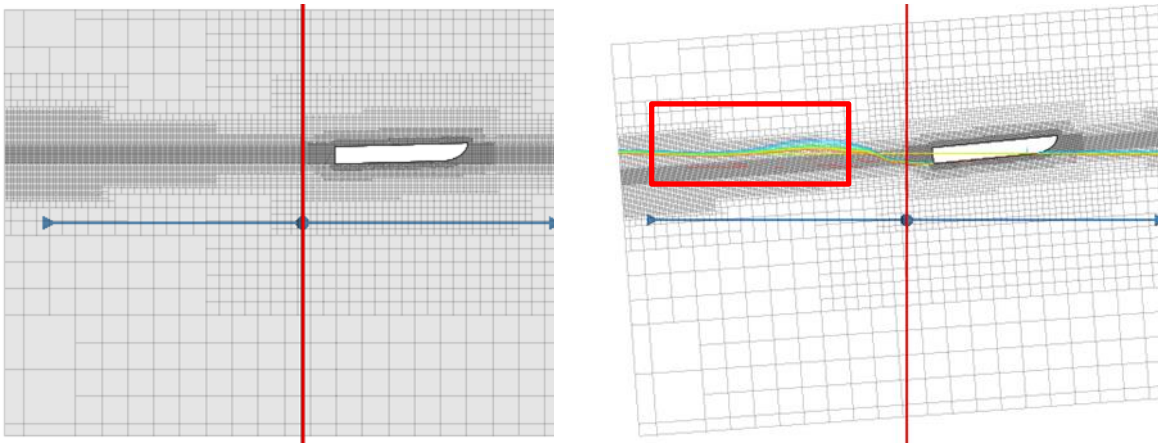

(a) (b)

Figure 11. Moving mesh (a) before analyzed (b) after analyzed

3.4 Benchmark

To compare the results of the mesh method, Fridsma's experimental data were used as validation with values of L/B = 5 and LCG = 0,6 L from AP 5 speeds were used based on the Froude number in the Fridsma experiment, namely 0,6; 0,9; 1,2; 1,5 and 1,8 (Table 1). Simulations were carried out with the same density so that the number of overset mesh was 1.462K, morphing mesh 684K, moving mesh 1.557K concentrated on the water surface and hull. The resistance was described by the non-dimensional unit R/Δ, where R was the drag and Δ was the displacement/ weight of the ship. The trim graph was expressed in units of degrees. Furthermore, the heave graph with non-dimensional units s/B with s was the displacement between the starting and ending points on the z-axis of the ship and B as the ship's width.

The resistance results obtained in this research were the difference between the CFD results and the Fridsma experiment, as shown in Figure 12. At low speeds, the morphing mesh method was closer to the Fridsma experiment, with an error of less than 4,5%. In the state of the hump overset mesh, it was closer to the experiment, with an error of less than 0,5%. Meanwhile, at high speed, the moving mesh method was close to the experiment, with an error of 8%.

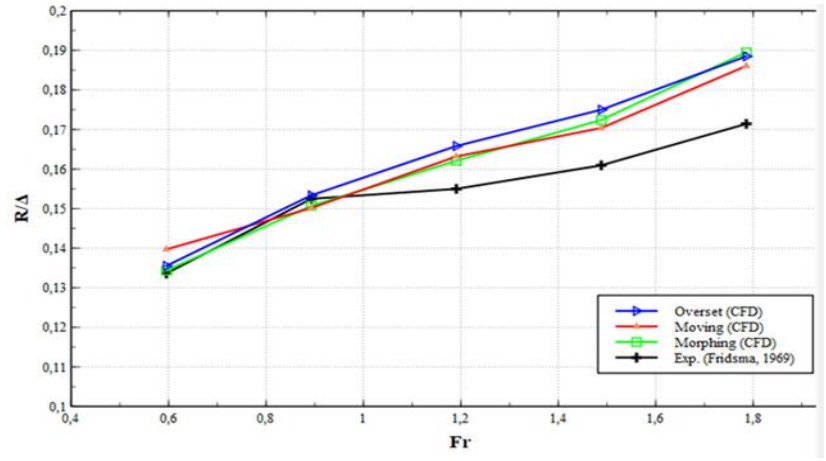

Figure 12. Resistance

From the trim graph in figure 13, there was a difference between the CFD results and the Fridsma experiment. In this research, the overset mesh results tended to approach the Fridsma experiment with a maximum error of 11%. At the same time, the morphing mesh or moving mesh tended to be less close to the Fridsma experiment, with a maximum error of 15%.

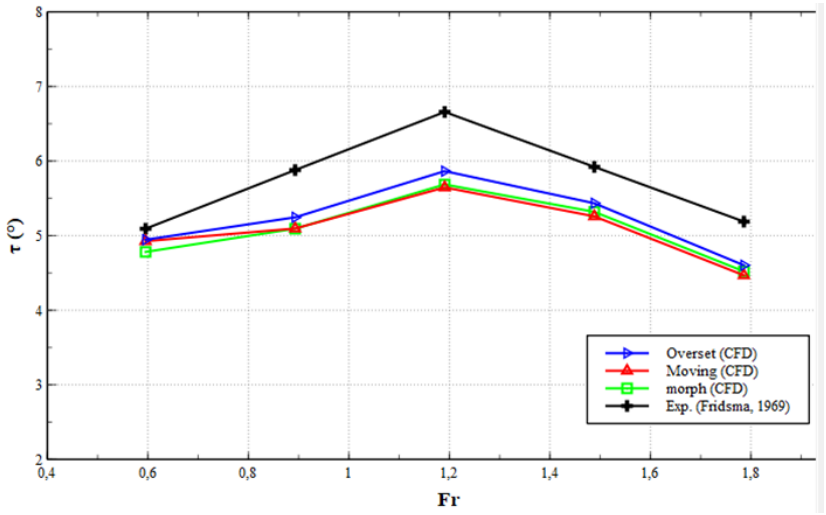

Figure 13. Trim

Based on the heave graph in figure 14, there was a difference between the CFD results and the Fridsma experiment. In this time, the moving mesh method at low speed obtained results that tended to approach the Fridsma experiment, with an error of 14%. In the hump state, the morphing mesh method approached the Fridsma experiment with an error of 11%. At high speed, the overset mesh method tended to approach the Fridsma experiment, with an error of 6%.

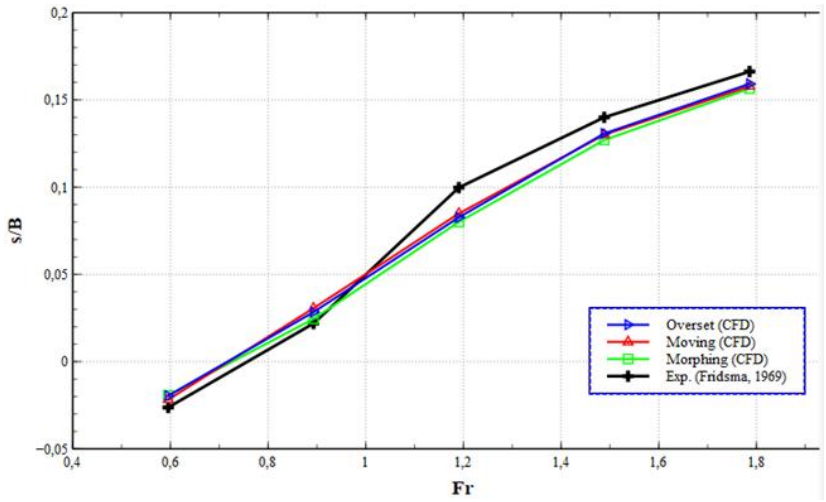

Figure 14. Heave

The results of the numerical simulation showed positive results when compared to the results of the Fridsma experiment. It can be seen from figure 12, figure 13, and figure 14. Although on the resistance and heave graph, there were a few inaccuracies in Fr 1,2 – Fr 1,8. In contrast, inaccuracies also occurred in the trim graph, namely at Fr 0,6 – Fr 1,8.
Research by Wheeler et al. in figure 15 performed a numerical simulation with the fridsma hull form. Wheeler's research had an error of 17,26% at Fr 1,78. Meanwhile, this research obtained an error of 15% at the same Fr. Hence, the results of this numerical simulation could be accepted.

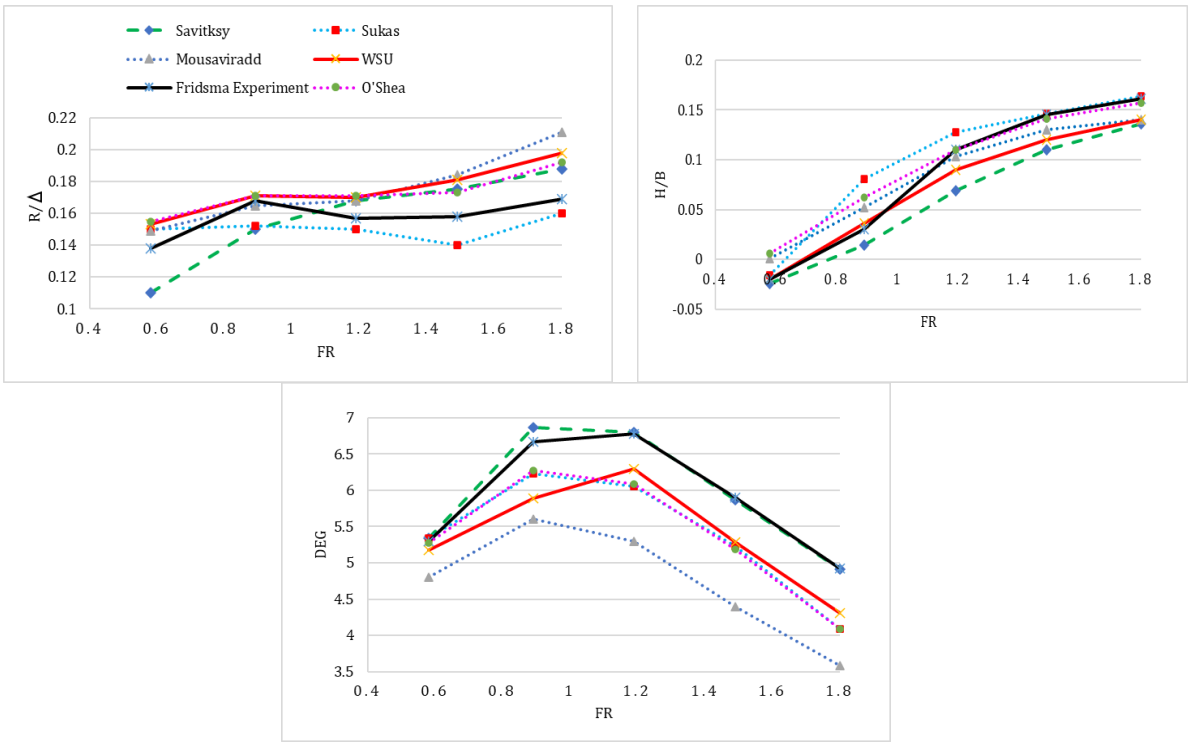

Figure 15. Comparison of drag, trim and heave [23]

In this research, the time-step used was 0.009 s. The time-step referred to the ITTC calculation. In addition, the function of the time-step was to speed up the convergence of a simulation. The simulation

could be ended when the graph had converged or had a relatively small difference in value (stagnant). Furthermore, the value taken was based on the average of the converged results. The overset mesh, morphing mesh, and moving mesh methods had different processing times to achieve convergence. Table 6 explains the time required to obtain convergent results from the three methods with the number of grids and times steps that were not too different. In Figure 16, it can be seen the difference in the processing time of each mesh method.

In this research obtained several characteristics of the overset mesh, morphing mesh, and moving mesh methods which were listed in the form of the advantages and disadvantages of the three methods, which are reported in Table 7. The advantages and disadvantages of the table did not guarantee accuracy due to differences in the ship characteristics.

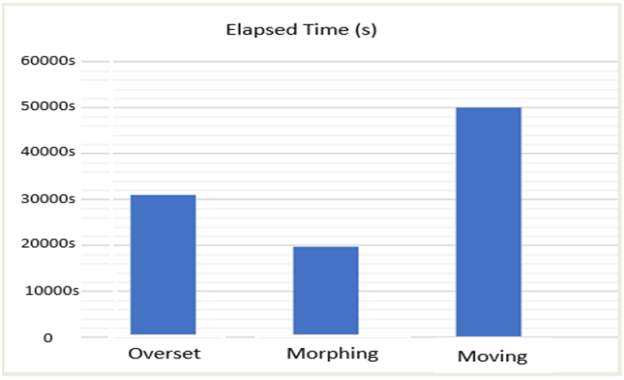

Figure 16. Comparison of processing time from each kind of mesh

Table 6. Time description

Parameters	Overset mesh	Morphing mesh	Moving mesh
Time of mesh (s)	31080	19821	50077
Solution Time	10	10	10
Sum of mesh	1.457.318	1.367.837	1.557.979

Table 7. Strategy mesh characteristics

Method	Advantages	Disadvantages
Overset mesh	• Tends to approach validation when analyzing at a minimum and maximum speed • When analyzing the trim, the results obtained are slightly closer to the validation or experiment.	• Take a long time to get analysis results • In this study, when analyzing the constraints of the overset mesh method, it was not so close to the validation or fridsma experiment.
Morphing mesh	• Tends to approach experimentation when analyzing resistance, trim, and trim at low speeds. • It does not take too long time to get the results of the analysis	• At low speeds the results obtained tend to approach the validation of the experiment, but at high speeds obtained are less close to the validation of the experiment.

Method	Advantages	Disadvantages
Moving mesh	• When analyzing resistance, trim, and heave at high speeds, the results obtained tend to be close to validation or experimentation.	• It takes a little longer to get the analysis results • At high speeds the results obtained tend to be close to validation or experimentation, while at low speeds the results are less close to validation or experimental

4. Conclusion

Based on the results of numerical analysis using the Computational Fluid Dynamics (CFD) method, some conclusions are obtained as follows:

1. The numerical computational validation based on CFD had relatively good accuracy compared to the experimental results of Fridsma in predicting the drag, trim, and heave of fast boats. The inaccuracy of the results occurred at Fr > 1.
2. Based on the time efficiency point of view, moving mesh took more time to get the analysis results, while overset mesh and morphing mesh took a long time in one analysis.
3. In this research, it was reported that overset mesh had better results than other mesh techniques.

References

[1] G. Fridsma, 1969, *A Systematic Study of The Rough-water Performance of Planing Boat* (Hoboken, New Jersey)

[2] R. Yousefi, R. Shafaghat, and M. Shakeri, 2013, Hy*drodynamic analysis techniques for high-speed planing hulls*, *Appl. Ocean Res*, **42**, pp. 105–113, doi: 10.1016/j.apor.2013.05.004.

[3] S. Samuel, A. Trimulyono, and A. W. B. Santosa, 2019, *Simulasi CFD pada kapal planing hull, Kapal J. Ilmu Pengetah. dan Teknol. Kelaut.*, **16**, pp. 123–128, doi: 10.14710/kapal.v16i3.26397.

[4] S. Samuel, A. Trimulyono, P. Manik, and D. Chrismianto, 2021, *A numerical study of spray strips analysis on fridsma hull form, Fluids*, **6**, p. 420, doi: 10.3390/fluids6110420.

[5] O. F. Sukas, O. K. Kinaci, F. Cakici, and M. K. Gokce, 2017, *Hydrodynamic assessment of planing hulls using overset grids," Appl. Ocean Res,* **65**, pp. 35–46,doi: 10.1016/j.apor.2017.03.015.

[6] M. E. Biancolini, I. M. Viola, and M. Riotte, 2014, *Sails trim optimisation using CFD and RBF mesh morphing, Comput. Fluids*, **93**, pp. 46–60, doi: 10.1016/j.compfluid.2014.01.007.

[7] S. Mancini, 2015, *The Problem of Verification and Validation Processes of CFD Simulations of Planing Hulls*,(Università Degli Studi Di Napoli Federico II)

[8] S. Samuel, D. J. Kim, A. Fathuddiin, and A. F. Zakki, 2021, *A numerical ventilation problem on fridsma hull form using an overset grid system, IOP Conf. Ser. Mater. Sci. Eng,* **1096**, no. 1, p. 012041, doi: 10.1088/1757-899x/1096/1/012041.

[9] M. E. Biancolini, 2011, *Mesh Morphing And Smoothing By Means Of Radial Basis Functions (RBF): A Practical Example Using Fluent And RBF Morph*, (Handbook. Res. Comput. Sci. Eng. Theory Pract) pp. 347–380, doi: 10.4018/978-1-61350-116-0.ch015.

[10] I. Viola, R. Flay, and R. Ponzini, 2012, *Edinburgh research explorer CFD analysis of the hydrodynamic performance of two candidate America ' s Cup AC33 hulls*," *Int. J. Small Cr. Technol,* **154**

[11] A. De Marco, S. Mancini, S. Miranda, R. Scognamiglio, and L. Vitiello, 2017, *Experimental and numerical hydrodynamic analysis of a stepped planing hull, Appl. Ocean Res,* **64**. pp. 135–154, doi: 10.1016/j.apor.2017.02.004.

[12] Savitsky, 1964, *Hydrodynamic design of planing hulls, Mar. Technol. SNAME*, **1**, pp. 71–95,
[13] O. M. Faltinsen, 2006, *Hydrodynamics of High-Speed Marine Vehicles,* (New York: Cambridge University Press)
[14] R. Marshall, 2002, *All about powerboats: Understanding Design and Performance,* (McGraw Hill Professional)
[15] F. Moukalled, L. Mangani, and M. Darwish, 2016, *The Finite volume method in computational fluid dynamics in fluid mechanics and its applications,* **113**, (Springer)
[16] B. Launder and D. Spalding, 1974, *The numerical computation of turbulent flows*, *Comput. Methods Appl. Mech. Eng*, **3**, pp. 269–289.
[17] P. Lotfi, M. Ashrafizaadeh, and R. K. Esfahan, 2015, N*umerical investigation of a stepped planing hull in calm water*, *Ocean Eng,* **94**, pp. 103–110, doi: 10.1016/j.oceaneng.2014.11.022.
[18] A. G. Avci and B. Barlas, *"An experimental and numerical study of a high speed planing craft with full-scale validation," J. Mar. Sci. Technol.*, vol. 26, no. 5, pp. 617–628, 2018, doi: 10.6119/JMST.201810_26(5).0001.
[19] ITTC, 2011, *Practical Guidelines for Ship CFD Applications*, *ITTC – Recomm. Proced. Guidel.* ITTC, pp. 1–8.
[20] S. Mancini, 2015, *The Problem of Verification and Validation Processes of CFD Simulations of Planing Hulls*, (Università Degli Studi Di Napoli Federico II)
[21] J. Y. Kang and B. S. Lee, 2010, *Mesh-based morphing method for rapid hull form generation CAD Comput. Aided Des,* **42**, no. 11, pp. 970–976, doi: 10.1016/j.cad.2009.07.001.
[22] A. Fathuddiin, S. Samuel, K. Kiryanto, and A. Widyandari, 2020, *Prediksi hambatan kapal dengan menggunakan metode overset mesh pada kapal planing hull*, *J. Rekayasa Hijau*, **4**, no. 1, pp. 24–34, doi: 10.26760/jrh.v4i1.24-34.
[23] C. P. Fabio De Luca, Simone Mancini, Salvatore Miranda, *"An Extended Verification and Validation Study of CFD Simulations for Planing Hulls," J. Sh. Res*, **60**, no. 2, pp. 101–108, 2016.
[24] T. Tang, 2005, *Moving mesh methods for computational fluid dynamics*, pp. 141–173, doi: 10.1090/conm/383/07162.
[25] M. P. Wheeler, K. I. Matveev, and T. Xing, 2018, *Validation study of compact planing hulls at pre-planing speeds*, *Am. Soc. Mech. Eng. Fluids Eng. Div. FEDSM*, **2**, pp. 1–8, doi: 10.1115/FEDSM2018-83091.